Structural Engineering and Mechanics, Vol. 43, No. 3 (2012) 395-410
DOI: http://dx.doi.org/10.12989/sem.2012.43.3.395

Identification and suppression of vibrational energy in stiffened plates with cutouts based on visualization techniques

Kai Li*[1], Sheng Li[2] and De-you Zhao[2]

[1]*China Ship Development and Design Center, Wuhan 430064, P.R. China*
[2]*State Key Laboratory of Structural Analysis for Industrial Equipment, School of Naval Architecture, Dalian University of Technology, Dalian 116024, P.R. China*

(Received February 9, 2010, Revised May 23, 2012, Accepted July 10, 2012)

Abstract. The visualizing energy flow and control in vibrating stiffened plates with a cutout are studied using finite element method. The vibration intensity, vibration energy and strain energy distribution of stiffened plates with cutout at different excitation frequencies are calculated respectively and visualized for the various cases. The cases of different size and boundaries conditions of cutouts are also investigated. It is found that the cutout or opening completely changes the paths and distributions of the energy flow in stiffened plate. The magnitude of energy flow is significantly larger at the edges near the cutout boundary. The position of maximum strain energy distribution is not corresponding to the position of maximum vibrational energy. Furthermore, the energy-based control using constrained damping layer (CDL) for vibration suppression is also analyzed. According to the energy distribution maps, the CDL patches are applied to the locations that have higher energy distribution at the targeted mode of vibration. The energy-based CDL treatments have produced significant attenuation of the vibration energy and strain energy. The present energy visualization technique and energy-based CDL treatments can be extended to the vibration control of vehicles structures.

Keywords: stiffened plates; cutout; visualization; energy control; constrained damping layer; finite element method

1. Introduction

Stiffened plates and shells structure with cutouts are commonly found built-up structural components in spacecrafts, aircrafts, land-based vehicles and marine vehicles. In these structures, cutouts or opens are required for practical purposes as access ports for mechanical and pipe systems, simply to reduce structural weight, and to serve as doors and Windows. Cutouts and stiffeners existing in plates present a greater challenge than simple continuous structures such as beams and plates because of complexity structural configurations, high stress/strain concentration and uncertain boundary conditions. It is very important to understand the vibration sources and transmission paths, energy sink locations and its frequency contents of stiffened plates with cutouts for vibration control to improve passenger comfort, minimize crew fatigue, and in the case of naval

*Corresponding author, Ph.D., Engineer, E-mail: kaili109@sina.com

vessels, to avoid detection.

Studies on the static and dynamic properties of structural elements with cutouts or holes have been reported extensively. The numerical method for computing the natural frequencies of rectangular plates with cutouts can be broadly classified into three categories, finite element and finite difference methods (Paramasivam 1973), and a semi-analytical approach based on the Rayleigh-Ritz method. Of the various discrete methods, the finite element method is by far the most widely used for this class of problems. The free vibration characteristics of unstiffened and longitudinally stiffened square panels with symmetrically square cutouts are investigated by Sivasubramonian *et al.* (1999) using the finite element method. Lam and Hung (1990) studied the vibrations of plates with stiffened openings using orthogonal polynomials and the partitioning method. Natural frequencies of simply supported and fully clamped plates with stiffened openings were presented. Lee and Lim (1992) carried out the analysis of simply supported isotropic and orthotropic square plates with a square cutout centrally placed subjected to in-plane forces. Recently, dynamic instability of stiffened plates with cutouts subjected to harmonic in-plane uniform edge loading has been studied by many researchers (Srivastava 2003, Patel 2007). To the best of author's knowledge, studies on the dynamic response characteristics of stiffened plates with cutouts from the energy flow point of view are scanty in the literature.

Vibration intensity method was first introduced by Noiseux (1970) and later developed by Pavic (1976) which is analogous to acoustic intensity in a fluid medium; it is the vibration power flow per unit cross-sectional area in elastic medium. The vibration intensity technique is an essential tool for locating and ranking vibration sources and sinks on structures. It can indicate the magnitude and direction of vibrational energy flow at any point of a mechanical structure at frequencies of interest (Gavric 1993, Hambric 1994). Vibration intensity field by plotting a vector map gives the particular information of energy flow transmission paths and positions of source and sinks of mechanical energy. Lee and Lim (2004) predicted the vibration intensity of a plate with multiple discrete and distributed dampers by the finite element method. Cieślik *et al.* (2006) presented the formulations for structural vibration intensity calculation involving the external loads and moments based on the complex modal analysis by finite element method. Furthermore, the vibration intensity vector filed was used for computing the vibration power flow pattern of plates with multiple cutouts (Khun 2003), composite plates with holes (Xu 2004). There were very few reports on the energy flow transmission and distribution of a stiffened plate with cutout using energy streamline technique.

Energy flow in a plate structure has been investigated by many researchers. Bernhard and Bouthier (1990) firstly developed a set of equations which govern the space and time averaged energy density in plates to investigate the mechanisms of energy generation, transmission and absorption. Further investigations of the energy model of plates proved that the vibration conduction equation is valid for the two-dimensional vibration field composed of plane wave components (Bernhard and Bouthier 1990, Ichchou 1996).

There are several techniques that can be used to suppress mechanical vibration and noise. Among them, the addition of damping is one of the most practical approaches over a wide range of applications. In particular, a surface treatment of constrained damping layer (CDL) on a structure is a conventional method to reduce structural vibrations or noises owing to the low cost and easy implementation of such a treatment. Constrained damping has a high loss factor because it dissipates energy during the shear deformation of viscoelastic materials generated by a constraining metal layer. These CDL patches should be minimized, as a reduction of weight generally results in both performance and economic benefits. Extensive efforts have been exerted in the past to optimally design CDL treatments subject to space or weight limitations (Plunkett and Lee 1970, Nakra 1998). In an effective treatment of damping materials, to determine the optimum locations for control of energy flow in vibrating plates becomes an important issue.

The aim of this study is to investigate the effects of cutout on the energy flow in stiffened plates subject to point force excitation using energy visualization technique. Furthermore, the optimum placement of CDL patches by energy-based control approach is determined. Simulation results show a significant attenuation of vibration energy level. This approach is proposed as a meaningful tool for the vibration control of vehicles structures.

2. Theory and formulation

2.1 Vibration intensity in plates

Gavric and Pavic (1993) developed equivalent structural vibration intensity algorithms that can be implemented both in the time domain and the frequency domain.

From plate theory, the vibration equation of a thin plate may be expressed as

$$D\left(\frac{\partial^4\zeta}{\partial x^4}+2\frac{\partial^4\zeta}{\partial x^2\partial y^2}+\frac{\partial^4\zeta}{\partial x^4}\right)+\rho h\frac{\partial^2\zeta}{\partial t^2}=f \tag{1}$$

Where $f = Fe^{i\omega t}$ is the external harmonic exciting force; $D = Eh^3/12(1-\mu^2)$

The instantaneous structural intensity at point (x, y) may be written as

$$P_x(x,y;t)=D\left[\dot{\zeta}\frac{\partial}{\partial x}\left(\frac{\partial^2\zeta}{\partial x^2}+\frac{\partial^2\zeta}{\partial y^2}\right)-\frac{\partial\dot{\zeta}}{\partial x}\left(\frac{\partial^2\zeta}{\partial x^2}+\mu\frac{\partial^2\zeta}{\partial y^2}\right)-(1-\mu)\frac{\partial\dot{\zeta}}{\partial y}\frac{\partial^2\zeta}{\partial x\partial y}\right]$$

$$P_y(x,y;t)=D\left[\dot{\zeta}\frac{\partial}{\partial y}\left(\frac{\partial^2\zeta}{\partial x^2}+\frac{\partial^2\zeta}{\partial y^2}\right)-\frac{\partial\dot{\zeta}}{\partial y}\left(\frac{\partial^2\zeta}{\partial y^2}+\mu\frac{\partial^2\zeta}{\partial x^2}\right)-(1-\mu)\frac{\partial\dot{\zeta}}{\partial x}\frac{\partial^2\zeta}{\partial y\partial x}\right] \tag{2}$$

Assuming the plate has a harmonic motion of frequency ω, its displacement may be expressed as

$$\zeta(x,y;t) = A(x,y)e^{i\omega t} \tag{3}$$

Where $A(x,y)$ is the response amplitude of the vibrating plate.

The strain distributions of the plate may be written as

$$\psi_x(x,y)=\frac{\partial^2 A(x,y)}{\partial x^2},\psi_y(x,y)=\frac{\partial^2 A(x,y)}{\partial y^2}\quad\text{and}\quad\psi_{xy}(x,y)=\frac{\partial^2 A(x,y)}{\partial x\partial y} \tag{4}$$

Substituting Eq. (3) and Eq.(4) into Eq. (2), the vibration intensity can be rewritten as

$$P_x(x,y;t)=D\left[\dot{\zeta}\frac{\partial}{\partial x}\left(\frac{\partial^2\zeta}{\partial x^2}+\frac{\partial^2\zeta}{\partial y^2}\right)-\frac{\partial\dot{\zeta}}{\partial x}\left(\frac{\partial^2\zeta}{\partial x^2}+\mu\frac{\partial^2\zeta}{\partial y^2}\right)-(1-\mu)\frac{\partial\dot{\zeta}}{\partial y}\frac{\partial^2\zeta}{\partial x\partial y}\right]$$

$$=i\omega D\left[\zeta\frac{\partial}{\partial x}(\psi_x(x,y)+\psi_y(x,y))-\frac{\partial\zeta}{\partial x}(\psi_x(x,y)+\mu\psi_y(x,y))-(1-\mu)\frac{\partial\zeta}{\partial y}\psi_{xy}(x,y)\right]e^{i2\omega t}$$

$$=P_X e^{i2\omega t}$$

$$P_y(x,y;t) = D\left[\dot{\zeta}\frac{\partial}{\partial y}\left(\frac{\partial^2\zeta}{\partial x^2}+\frac{\partial^2\zeta}{\partial y^2}\right)-\frac{\partial\dot{\zeta}}{\partial y}\left(\frac{\partial^2\zeta}{\partial y^2}+\mu\frac{\partial^2\zeta}{\partial x^2}\right)-(1-\mu)\frac{\partial\dot{\zeta}}{\partial x}\frac{\partial^2\zeta}{\partial y\partial x}\right]$$

$$= i\omega D\left[\zeta\frac{\partial}{\partial y}(\psi_x(x,y)+\psi_y(x,y))-\frac{\partial\zeta}{\partial y}(\psi_y(x,y)+\mu\psi_x(x,y))-(1-\mu)\frac{\partial\zeta}{\partial x}\psi_{xy}(x,y)\right]e^{i2\omega t}$$

$$= P_Y e^{i2\omega t} \tag{5}$$

Where

$$P_X = i\omega D\left[\zeta\frac{\partial}{\partial x}(\psi_x(x,y)+\psi_y(x,y))-\frac{\partial\zeta}{\partial x}(\psi_x(x,y)+\mu\psi_y(x,y))-(1-\mu)\frac{\partial\zeta}{\partial y}\psi_{xy}(x,y)\right]$$

and $P_Y = i\omega D\left[\zeta\frac{\partial}{\partial y}(\psi_x(x,y)+\psi_y(x,y))-\frac{\partial\zeta}{\partial y}(\psi_y(x,y)+\mu\psi_x(x,y))-(1-\mu)\frac{\partial\zeta}{\partial x}\psi_{xy}(x,y)\right]$

may be considered as the amplitudes of structural power flow.

The structural intensity gradients may be expressed as

$$\frac{\partial P_x}{\partial x} = \frac{\partial}{\partial x}P_X e^{i2\omega t} \quad \text{and} \quad \frac{\partial P_y}{\partial y} = \frac{\partial}{\partial y}P_Y e^{i2\omega t} \tag{6}$$

Streamline visualization technique (Xu 2005) is a very useful tool to represent the transmission direction of a vector field. This technique is widely used in computer graphics flow visualization in fluid mechanics to display the vector field of the fluid flow. The velocity vector at any point of one streamline is tangent to that line. Up until the last decade the studies of sound flow visualization are rather seldom in the structural acoustical practice. The vibration intensity field is also a vector field representing the structural energy flow in a structure. Thus, this technique can show the energy transmission paths and indicate the vibration source and energy sinks. Based on the general fluid mechanics definition, the vibration intensity streamline can be similarly expressed as

$$dr \times P(r,t) = 0 \tag{7}$$

Where r is an energy flow particle position. The cross product can be given by

$$\begin{vmatrix} i & j & k \\ P_x & P_y & P_z \\ dx & dy & dz \end{vmatrix} = 0 \tag{8}$$

For a 2-D plate, the vibration intensity streamline is written as

$$\frac{dx}{P_x} = \frac{dy}{P_y} \tag{9}$$

2.2 Energy distribution in plates

The energy in a vibrating plate is the sum of the kinetic and potential energy. The distribution of the instantaneous kinetic energy of the plate may be expressed as

$$T = \frac{\rho h}{2}\left(\frac{\partial \zeta}{\partial t}\right)^2 = -\frac{1}{2}\rho h \omega^2 A^2 e^{i2\omega t} = T_A e^{i2\omega t} \tag{10}$$

Where $T_A = -\frac{1}{2}\rho h \omega^2 A^2$ may be considered as the amplitudes of structural kinetic energy.

The distribution of the instantaneous strain energy of the plate may be expressed using Eq. (3) as

$$\begin{aligned} U &= \frac{D}{2}\left[\left(\frac{\partial^2 \zeta}{\partial x^2}\right)^2 + \left(\frac{\partial^2 \zeta}{\partial y^2}\right)^2 + 2\mu \frac{\partial^2 \zeta}{\partial x^2}\frac{\partial^2 \zeta}{\partial y^2} + 2(1-\mu)\left(\frac{\partial^2 \zeta}{\partial x \partial y}\right)^2\right] \\ &= \frac{D}{2}\left[\left(\frac{\partial^2 A}{\partial x^2}\right)^2 + \left(\frac{\partial^2 A}{\partial y^2}\right)^2 + 2\mu \frac{\partial^2 A}{\partial x^2}\frac{\partial^2 A}{\partial y^2} + 2(1-\mu)\left(\frac{\partial^2 A}{\partial x \partial y}\right)^2\right] e^{i2\omega t} \\ &= U_A e^{i2\omega t} \end{aligned} \tag{11}$$

Where $U_A = \frac{D}{2}\left[\left(\frac{\partial^2 \zeta}{\partial x^2}\right)^2 + \left(\frac{\partial^2 \zeta}{\partial y^2}\right)^2 + 2\mu \frac{\partial^2 \zeta}{\partial x^2}\frac{\partial^2 \zeta}{\partial y^2} + 2(1-\mu)\left(\frac{\partial^2 \zeta}{\partial x \partial y}\right)^2\right]$ may be considered as the amplitudes of structural strain energy.

Then, the instantaneous energy flow of the plate can be written as

$$E = T + U = T_A e^{i2\omega t} + U_A e^{i2\omega t} = (T_A + U_A) e^{i2\omega t} \tag{12}$$

Strain energy has been increasingly adopted to detect and locate damages in engineering structures, in the finite element formulation, the stain energy over a discrete pate of an undamped structure vibrating in its *r*th mode is yield by the following quadratic form pertaining to any finite element

$$U^{(r)} = \{\psi\}_r^T [K_e] \{\psi\}_r \tag{13}$$

Where r denotes the mode number, $U^{(r)}$ is strain energy, $\{\psi\}_r$ is the eigenvector of finite element with the vector elements represented by all the value of nodal coordinates of the element, $\{\psi\}_r^T$ is the transpose of the eigenvector $\{\psi\}_r$, $[K_e]$ is the stiffness matrix of the element.

2.3 Relationship between the structural vibration intensity and the vibration energy

The structural intensity can be related to the instantaneous energy stored in the pate in the following. The instantaneous energy flow of the plate can be written as

$$E = T + U = T_A e^{i2\omega t} + U_A e^{i2\omega t} = (T_A + U_A) e^{i2\omega t} \tag{14}$$

$$\frac{\partial E}{\partial t} = -i\omega \left\{ \rho h \omega^2 A^2 - D\left[\left(\frac{\partial^2 A}{\partial x^2}\right)^2 + \left(\frac{\partial^2 A}{\partial y^2}\right)^2 + 2\mu \frac{\partial^2 A}{\partial x^2}\frac{\partial^2 A}{\partial y^2} + 2(1-\mu)\left(\frac{\partial^2 A}{\partial x \partial y}\right)^2\right]\right\} e^{i2\omega t} \tag{15}$$

Using Eq. (5), the sum of the structural intensity gradients can be express as

$$\frac{\partial P_x}{\partial x}+\frac{\partial P_y}{\partial y}=\left(\frac{\partial}{\partial x}P_X+\frac{\partial}{\partial y}P_Y\right)e^{i2\omega t}==-i\omega D\left(\frac{\partial^4 A}{\partial x^4}+2\frac{\partial^4 A}{\partial x^2\partial y^2}+\frac{\partial^4 A}{\partial x^4}\right)e^{i2\omega t}$$
$$+iwD\left[\left(\frac{\partial^2 A}{\partial x^2}\right)^2+\left(\frac{\partial^2 A}{\partial y^2}\right)^2+2\mu\frac{\partial^2 A}{\partial x^2}\frac{\partial^2 A}{\partial y^2}+2(1-\mu)\left(\frac{\partial^2 A}{\partial x\partial y}\right)^2\right]e^{i2\omega t} \quad (16)$$

Eq. (16) can be rewritten using Eq. (1) as

$$\frac{\partial P_x}{\partial x}+\frac{\partial P_y}{\partial y}=-i\omega\left\{\rho h\omega^2 A^2-D\left[\left(\frac{\partial^2 A}{\partial x^2}\right)^2+\left(\frac{\partial^2 A}{\partial y^2}\right)^2+2\mu\frac{\partial^2 A}{\partial x^2}\frac{\partial^2 A}{\partial y^2}+2(1-\mu)\left(\frac{\partial^2 A}{\partial x\partial y}\right)^2\right]\right\}e^{i2\omega t}-iwFe^{i2\omega t} \quad (17)$$

Using Eq. (15) and Eq. (17), the relationship of energy equation of a plate can be expressed as

$$\frac{\partial E}{\partial t}=\frac{\partial P_x}{\partial x}+\frac{\partial P_y}{\partial y}+iwfe^{i\omega t} \quad (18)$$

In particular, away from the exciting force, the Eq. (18) can be written as

$$\frac{\partial E}{\partial t}=\frac{\partial P_x}{\partial x}+\frac{\partial P_y}{\partial y} \quad (19)$$

3. Numerical results and discussions

3.1 Numerical models

Finite element method has been used as an efficient tool for modeling of the vibration response of the plate. In the present work, the undamped structural plate and its stiffeners are modelled using a mesh of eight-node isoparametric quadratic element with five degrees of freedom. The finite element model is analyzed using the commercial finite element software ANSYS. Consecutively a self-developed Matlab program is used for the post-process calculations.

3.2 Frequency parameters of stiffened plate with different cutout

It is frequently to position additional reinforcement around the opening to ensure that the strength lost by the cutouts. In the present paper, the stiffened plate is reinforced at the four edges of the cutout. The structural model used in this study is shown in Fig. 1. The finite element mesh for reinforced plate is shown in Fig. 2, also the stiffeners and plate are modeled by the shell element. The material properties are listed in Table 1. The effects of size and reinforcement of the cutout on the natural frequencies for different modes of free vibration are shown in Fig. 3. The frequencies of mode 1 and mode 4 continue to decrease without the opening edges reinforced at the same size of

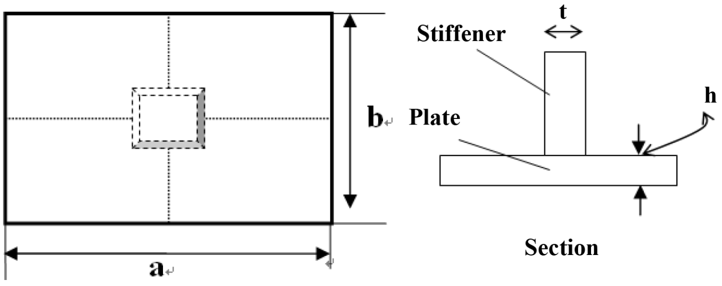

Fig. 1 Structural model

Table 1 Parameters of stiffened plate

Poisson's ratio	0.3
Young's modulus	210 GPa
Density	7800 kg/m^3
Thickness of plate	0.004 m
Height of stiffener	0.05 m
Width of stiffener	0.005 m

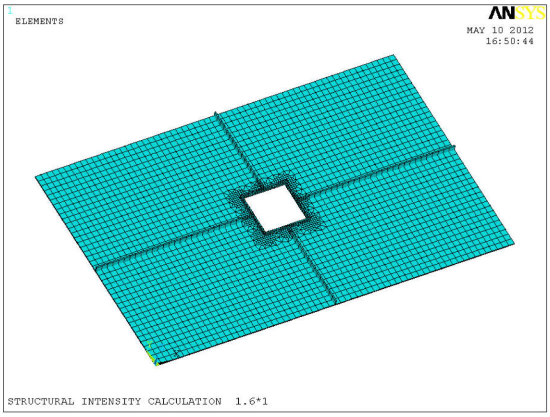

Fig. 2 Finite element mesh

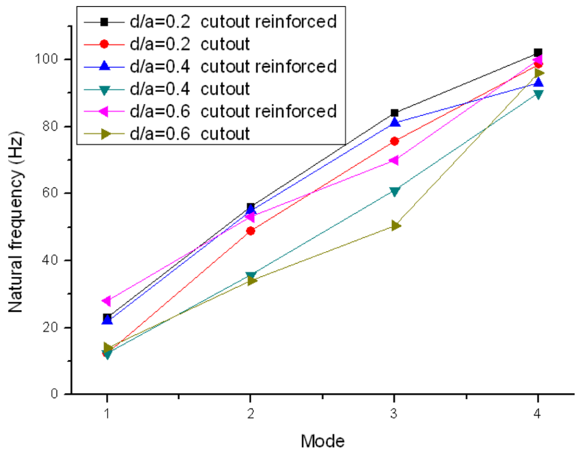

Fig. 3 Frequency parameters for a stiffened plate with cutout

cutout. It is observed that, there is a tendency of decrease in the natural frequencies in mode 2 and mode 3 with the increase in size of the cutout.

3.3 The effects of excitation frequency

In this section, the stiffened plate is simply supported along the four edges. The cutout is reinforced at the four edges. The finite element meshes are refined near the cutout edges and a higher order mesh refinement is used at the cutout corner in order to obtain sufficient accuracy of the stress and displacement predications. In order to investigate the vibratory energy flows in the stiffened plates with cutout, a corresponding external damper will be attached on the other side of the plate. The additional damper represents the presence of the dissipative element which can be used to simulate some particular structures such as the loosed bolt on board. The excitation point force with an amplitude of 1000 N is applied at x = 0.3 m and y = 0.3 m on the plate, an external damper with a damping rate of 100 Ns/m is attached to the plate at x = 1.3 m and y = 0.7 m.

The vibration intensity components are calculated for excitation frequencies corresponding to the nature frequencies of the stiffened plate with cutout to examine whether there were differences due to the excitation frequency on the energy transmission. Furthermore the total energy flow and modal strain energy are calculated based on the Eqs. (12)-(13) presented in Section 2. The visualization energy flow results at different excitation frequencies are shown in Figs. 4-7.

In order to account for the influences of excitation frequency, the diagrams for the four excitation frequencies are drawn respectively. Figs. 4(a), 4(b) and 4(c) present the vector of vibration intensity, vibration energy density and modal strain energy distribution map of stiffened plate with cutout at the excitation frequency of mode 1. Fig. 5, Fig. 6 and Fig. 7 show the same series of diagrams as in Fig. 4 at different excitation modes. From Fig. 4(a) it can be found that the patterns of energy flow are quite identical. The positions of the energy source and sink can be identified for stiffened plate with cutout, and the main flow of energy is in a direct path from force point to the damper. A small amount of energy flow is also shown reflected on the stiffeners and boundaries of plate.

With increasing frequency, the vibration energy transmission paths become more complex as in Figs. 5(a), 6(a) and 7(a), it can be seen in these figures that the energy flow patterns are changed with the variation of excitation modes, and the nature of vibration intensity field is frequency dependent. When a cutout is present, the intensity vectors are turned away from their normal path directing toward the cutout boundary. We can see that the direct energy flow, together with the reflection flow by the edges make many vortices and curls in the field for some cases. The phenomenon of vortex energy flow can also be shown clearly in Fig. 7(a). Energy vortices indicate relative amounts of energy in the stiffened plate. When the energy flow reaches the boundary, the vibration intensity is reflected and some virtual sources or sinks can be constructed. So it is difficult to diagnose the real source of vibration only by the energy vector maps.

Figs. 4(b)-7(b) clearly show that the energy flow distributes from the force input location through the stiffened plate with cutout at different excitation frequencies. The density of energy flow is significantly larger at the edges near the cutout boundary. The positions of maximum for these cases are almost same. Figs. 4(c)-7(c) also represent the contour plots of the magnitude of modal strain energy. The highest strain energy is located near the force excitation point and cutout edges for most cases. Comparing Figs. 4-7, we can find that under dynamic loading actions, the maximum value of strain energy does not indicate the maximum magnitude of vibration energy as the later is a product of kinetic energy and potential energy. It also means the locations of maximum vibration energy are not corresponding to the locations of maximum strain energy.

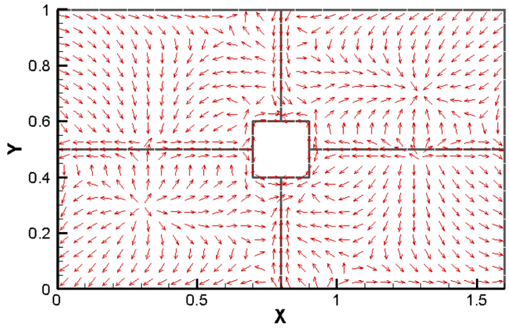

(a) Vector map Mode 1

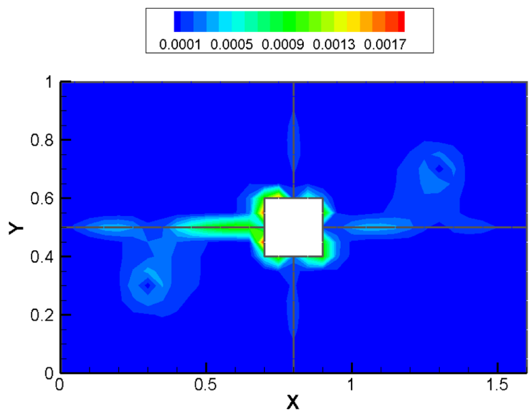

(b) Vibration energy distribution Mode 1

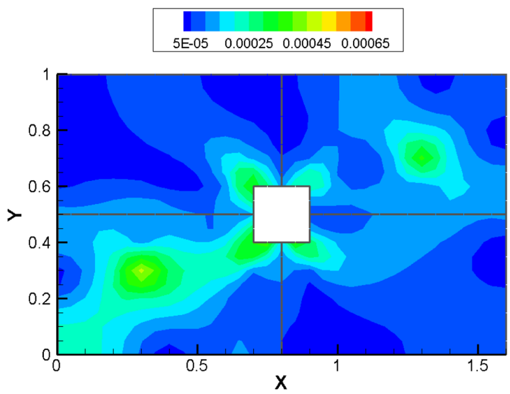

(c) Elastic strain energy Mode 1

Fig. 4 Stiffened plate with reinforced cutout, Mode 1, $d/a = 0.2$

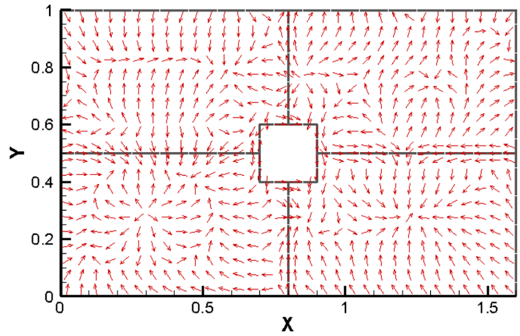

(a) Vector map Mode 2

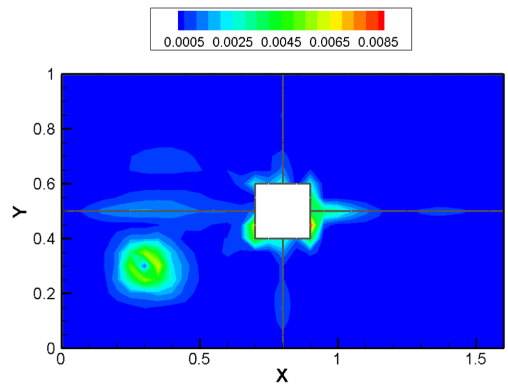

(b) Vibration energy distribution Mode 2

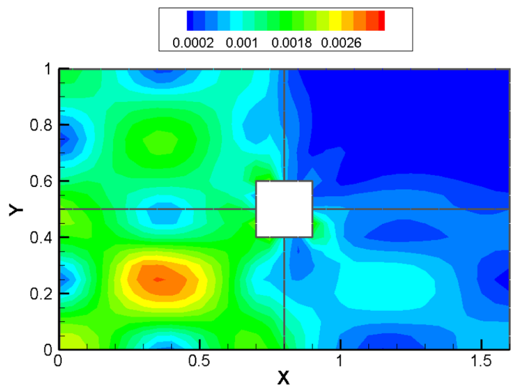

(c) Elastic strain energy Mode 2

Fig. 5 Stiffened plate with reinforced cutout, Mode 2, $d/a = 0.2$

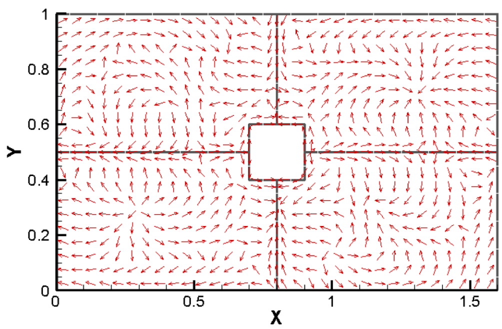

(a) Vector map Mode 3, *d*/*a*=0.2

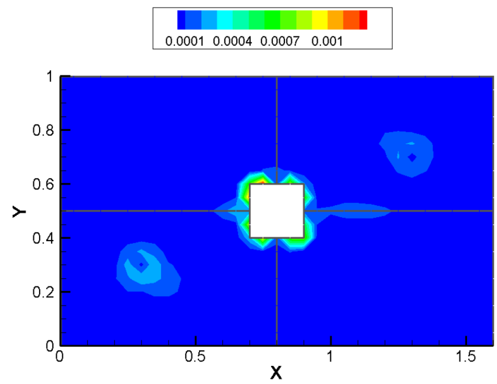

(b) Vibration energy distribution Mode 3, *d*/*a*=0.2

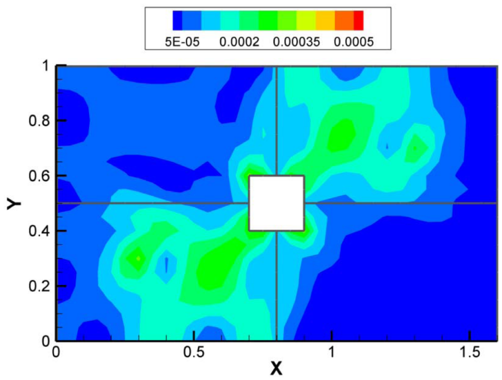

(c) Elastic strain energy Mode 3, *d*/*a*=0.2

Fig. 6 Stiffened plate with reinforced cutout, Mode 3, *d*/*a* = 0.2

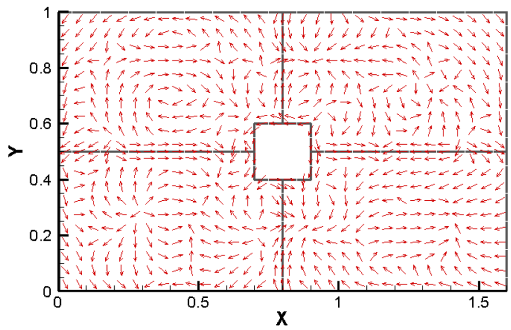

(a) Vector map Mode 4, *d*/*a*=0.2

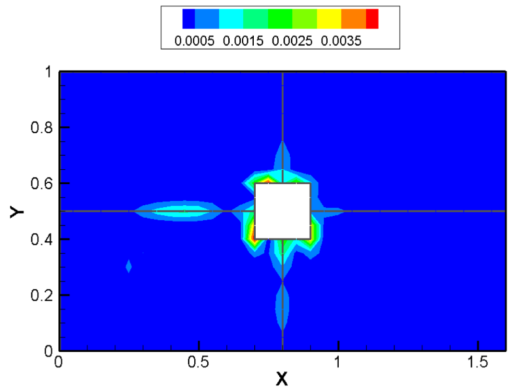

(b) Vibration energy distribution Mode 4, *d*/*a*=0.2

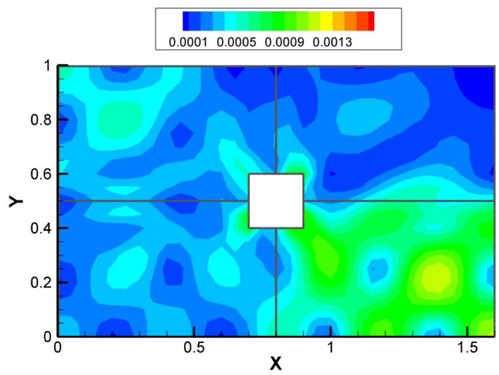

(c) Elastic strain energy Mode 4, *d*/*a*=0.2

Fig. 7 Stiffened plate with reinforced cutout, Mode 4, *d*/*a* = 0.2

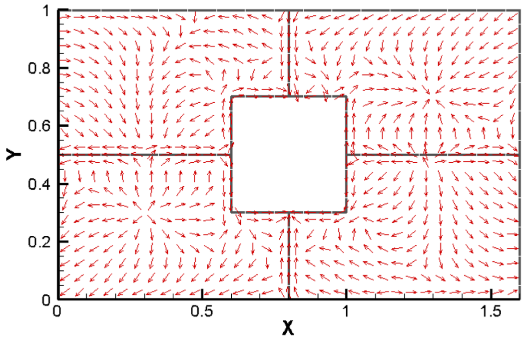

(a) Vector map Mode 1, *d/a*=0.4

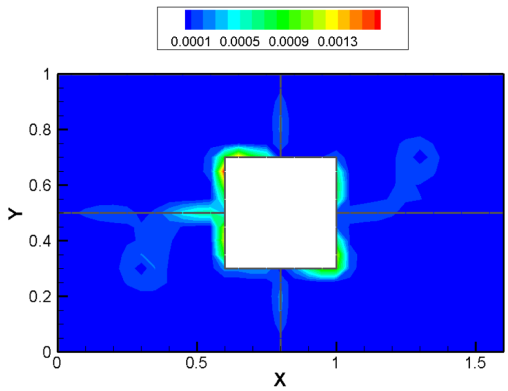

(b) Vibration energy distribution Mode 1, *d/a*=0.4

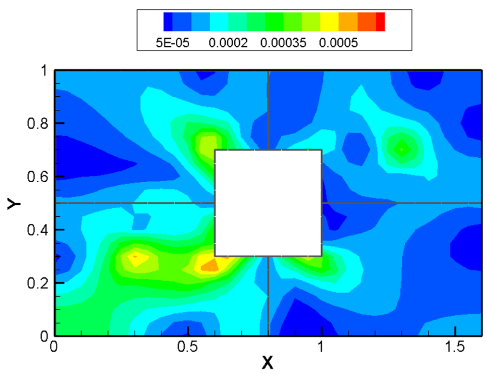

(c) Elastic strain energy Mode 1, *d/a*=0.4

Fig. 8 Stiffened plate with reinforced cutout, Mode 1, *d/a* = 0.4

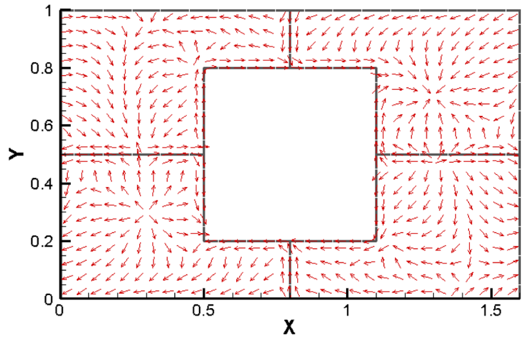

(a) Vector map Mode 1, *d/a*=0.6

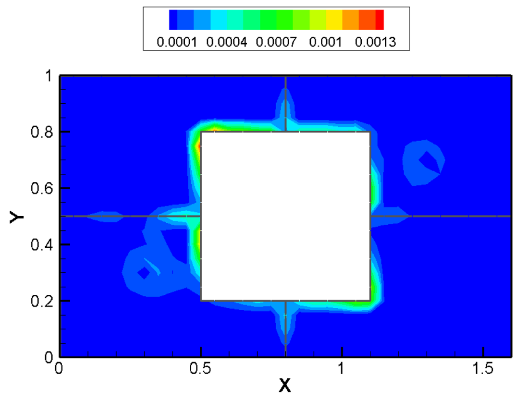

(b) Vibration energy distribution Mode 1, *d/a*=0.6

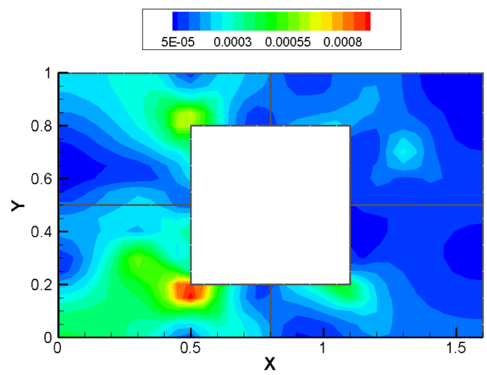

(c) Elastic strain energy Mode 1, *d/a*=0.6

Fig. 9 Stiffened plate with reinforced cutout, Mode 1, *d/a* = 0.6

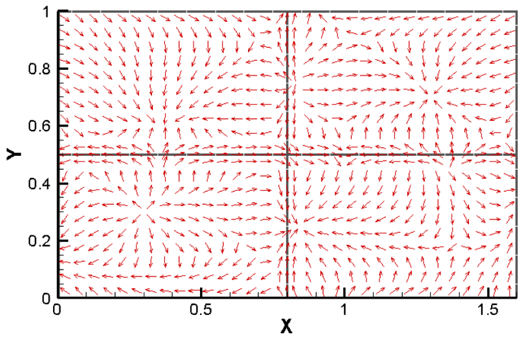

(a) Vector map Mode 1

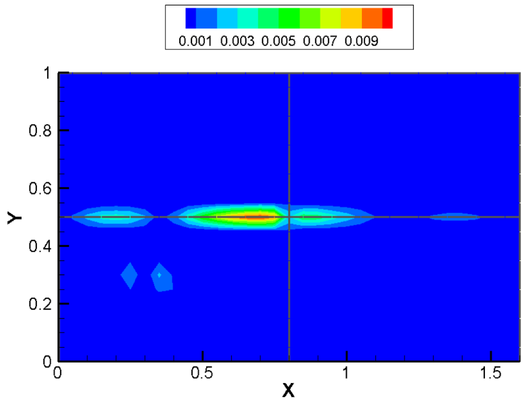

(b) Vibration energy density Mode 1

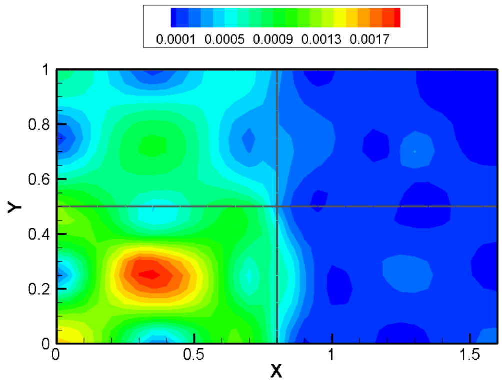

(c) Elastic strain energy

Fig. 10 Stiffened plate without cutout, Mode 1

3.4 The effects of cutout size

In this study, the emphasis is on the influence of the cutout size to the energy flow in plate. In order to account for this, the diagrams for the excitation frequency near the first structural resonance are drawn respectively. The energy vector, vibration energy density and modal strain energy distribution in plate are visualized and compared to analyze the effect of various cutout sizes on the stiffened plate. The geometrical setup, boundary conditions, material properties and loading conditions carried out in this simulation are the same as in the previous example, where the cutout size ratios are selected as the variables.

The stiffened plate with different cutout size ratios d/a = 0.2, d/a = 0.4 and d/a = 0.6 are considered and plotted as shown in Fig. 4 and Figs. 8-9. In order to reveal the influence of cutout existence on the energy flow, the energy vector, vibration energy density and modal strain energy distribution in stiffened plate without cutout are also illustrated in Figs. 10(a)-(c) respectively.

Comparing Fig. 4, Fig. 8, Fig. 9 and Fig. 10, we can find that the patterns of energy flow are changed by the variation of cutout size. The existence of a cutout in the plate completely changes the energy vector, and so does the pattern of energy flow distributions in the plate. It indicates that there is a slight difference in the energy flow paths between the various cutout sizes. The energy flow path does not transmit directly from the source to the sink any more. There exist several vortices of energy flow near the edge of cutout in the stiffened plate for some case. It is more significant when the greater energy concentration occurs along the cutout edges in Fig. 4(b), Fig. 8(b) and Fig. 9(b). It can be seen in these figures that the energy distribution patterns are changed near the cutout boundary.

Three modal strain energy with different cutout sizes are also considered and the results are shown in Fig. 4(c), Fig. 8(c) and Fig. 9(c). It is evident that the size of a cutout also changes the distributions of strain energy in stiffened plate. The strain energy concentration regions are still near the edge of the cutout, but not the same positions for most cases.

From Fig.4 and Figs. 8-10, we can find that under dynamic force excitation, the maximum value of strain energy does not indicate the maximum magnitude of vibration energy. The regions of high concentration of strain energy are exposed to the risk of damage. According to these results, the patterns of vibration energy and the modal strain energy are important in considering the positions to control the energy flow in a structure.

4. Energy-based strategy for vibration suppression

Control of structural vibration is usually based on either a modal description or an energy description of the structure. The energy-based approach is more appropriate to control the energy transmission from one area of the structure to another area. The advantage of choosing energy-based strategy rather than the strategy of minimizing the transverse acceleration achieves a better control performance (Cremer 2005, P. AUDRAIN 2000).

The structural vibration energy transmission and distribution enable the investigation in the regions of high concentration of strain energy which is exposed to the fatigue failure of structure. It can be considered as the identification of the regions for application of additional viscoelastic damping in purpose of lowering of vibration energy transmission and strain concentration.

The damping layer is assumed to be linearly viscoelastic with their constitutive equations described using the complex modulus approach in the frequency domains.

$$E^*(\omega) = E'(\omega) + iE''(\omega) = E'(\omega)(1 + i\eta) \tag{20}$$

Where $E'(\omega)$ and $E''(\omega)$ are called the storage modulus and loss modulus respectively.

Table 2 Material properties of the constrained viscoelastic damping layer

Parameters	Constraining Layer	Viscoelastic Layer
Young's modulus, N/m^2	6.9E+10	1.794E+6
Posson's ratio	0.3	0.3
Density, kg/m^3	2700	960
Loss factor		0.5
Thickness, mm	1.5	12

A partial constrained-layer damping patch on a base plate is shown in Fig. 11. In finite element approach simulation, the CDL patches are modeled by solid elements with different Young's modulus, Poisson's ratio, loss factor and density listed in Table 2. In order to investigate the pure energy sink in the stiffened plate with cutout, no external damper is attached on the other side of the plate.

According to the energy distribution maps, the CDL patches are then applied to the untreated

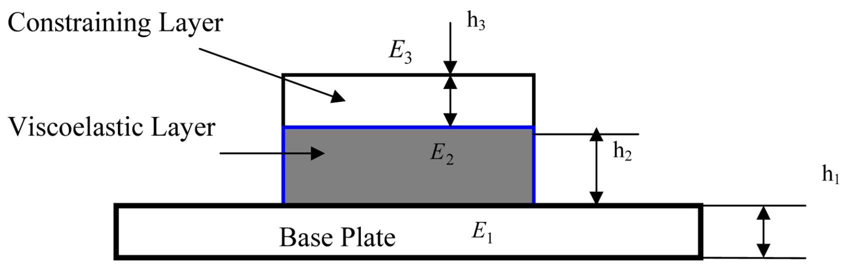

Fig. 11 Constrained damping layer plate

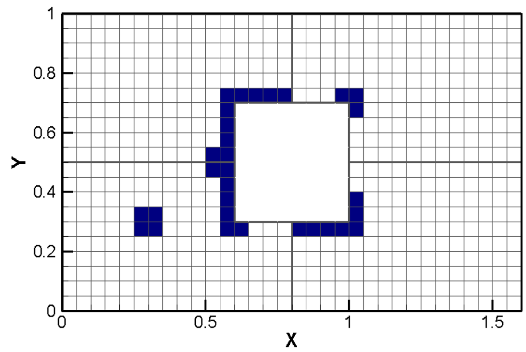

Fig. 12 The locations of CDL patches

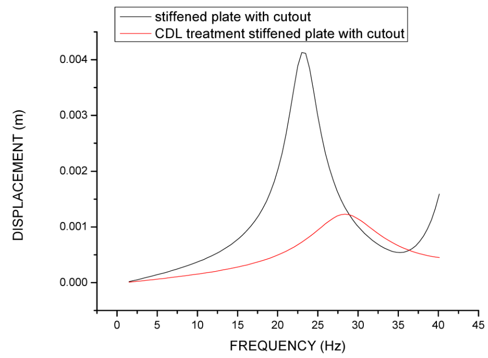

Fig. 13 Numerical comparison of frequency response curves

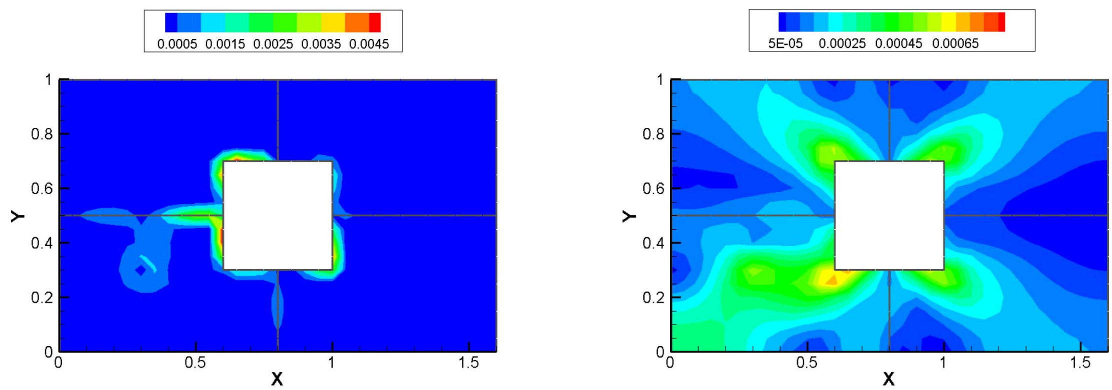

Fig. 14 The plots of vibration energy distribution and the modal strain energy untreated pattern

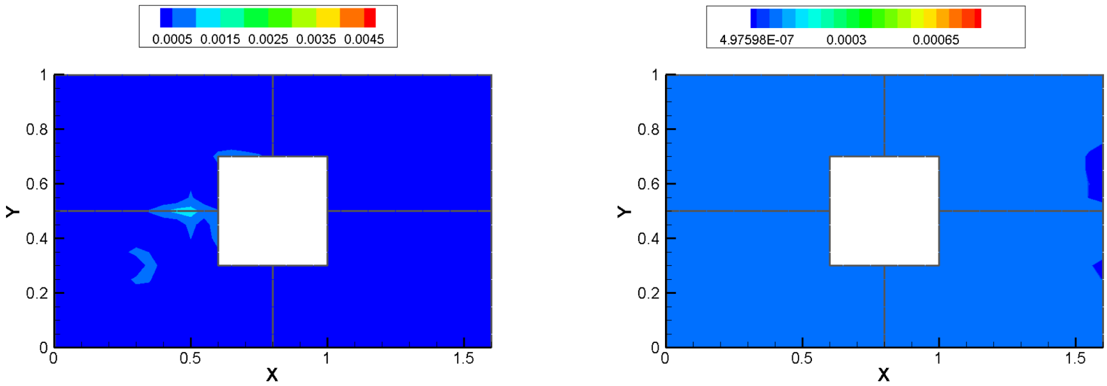

Fig. 15 The plots of vibration energy distribution and the modal strain energy CDL treated pattern

element that has higher energy distribution at the targeted mode of vibration as shown in Fig. 12. Fig. 13 presents the simulation-based frequency response curve for the untreated and CDL patches treated plate pattern. The maximum response of displacement of the stiffened plate with cutout decreases by 70% with the energy-based treated pattern. Fig. 14 presents the locations of vibration energy and strain energy concentrations. Fig. 15 shows the controlled CDL/plate system, for the vibration energy density of treated plate pattern and for the modal strain energy of treated plate pattern. It is observed from the color plots that CDL treatments have produced significant attenuation of the vibrational energy and strain energy. The maximum of vibration energy density and strain energy are attenuated by 57% and 65% respectively. Simulation results show a great reduction of vibration energy level.

5. Conclusions

The vibration energy flow and control of stiffened plates with cutout are studied in this paper. The main conclusions of this study can be summarized in the following three points:

(1) The energy transmission paths of stiffened plate with cutout are very complex and frequency dependent and at some cases closure vortex fields appear. The existence of a cutout in the stiffened plate completely changes the energy vectors, and so does the pattern of energy flow distributions in the plate.

(2) The cutout completely changes the distributions of the vibration energy and strain energy in stiffened plate. The magnitude of energy flow is significantly larger at the edges near the cutout boundaries. Moreover the position of maximum strain energy distribution is not identical to the position of maximum vibrational energy. The regions of high concentration of strain energy are exposed to the risk of damage. According to this, the patterns of vibration energy and the modal strain energy are both important in considering the positions to control the energy flow in a vibrating structure.

(3) CDL attached on a structural surface is very effective in reducing structural vibration. According to the energy distribution maps, the CDL patches should be applied to places where the stiffened plate has higher energy distribution. It gains a significant attenuation of the

vibrational energy and structure response. The application of the energy visualization technique has improved the quality of structure-borne noise diagnostics, while energy based-control approach is effective for the vibration control of marine structures.

References

Audrain, P., Masson, P. and Berry, A. (2000), "Investigation of active structural intensity control in finite beams: theory and experiment", *J. Acoust. Soc. Am.,* **108**, 612-623.

Bernhard, R.J. and Bouthier, O. (1990), "Model of the space averaged energetics of plates", *Proceedings of the AIAA 13th Aero-acoustics Conference*, Tallahassee, FL.

Bouthier, O. and Bernhard, R.J. (1995), "Simple models of energy flow in vibrating plates", *J. Sound Vib.*, **182**, 149-164.

Cieœlik, J. and Bochniak, W. (2006), "Vibration energy flow in ribbed plates", *Mechanics*, **25**(3), 119-123.

Cremer, L., Heckl, M. and Ungar, E.E. (2005), *Structure-borne Sound*, Second Edition, Springer-Verlag, Berlin.

Gavric, L. and Pavic, G. (1993), "A finite element method for computation of vibration intensity by the normal mode approach", *J. Sound Vib.*, **164**(1), 29-43.

Hambric, S.A. and Taylor, P.D. (1994), "Comparison of experimental and finite element structure-borne flexural wave power measurements for straight beam", *J. Sound Vib.*, **170**(5), 595-605.

Khun, M.S., Lee, H.P. and Lim, S.P. (2003), "Computation of structural intensity for plates with multiple cutouts", *Struct. Eng. Mech.,* **16**(5), 627-641.

Khun, M.S., Lee, H.P. and Lim, S.P. (2004), "Structural intensity in plates with multiple discrete and distributed spring-dashpot systems", *J. Sound Vib.*, **276**(3), 627-648.

Lam, K.Y. and Hung, K.C. (1990), "Vibration study on plates with stiffened openings using orthogonal polynomials and partitioning method", *Comput. Struct.*, **33**(3), 295-301.

Lee, H.P. and Lim, S.P. (1992), "Free vibration of isotropic and orthotropic square plate with square cutouts subjected to in plane forces", *Comput. Struct.,* **43**, 431-437.

Nakra, B.C. (1998), "Vibration control in machines and structures using viscoelastic damping", *J. Sound Vib.*, **211**(3), 449-465.

Noiseux, D.U. (1970), "Measurement of power flow in uniform beams and plates", *J. Acoust. Soc. Am.*, **47**(1), 238-247.

Paramasivam, P. (1973), "Free vibration of square plates with square openings", *J. Sound Vib.*, **30**(2), 173-178.

Patel, S.N., Datta, P.K. and Sheikh, A.H. (2007), "Dynamic instability analysis of stiffened shell panels subjected to partial edge loading along the edges", *Int. J. Mech. Sci.*, **49**, 1309-1324.

Pavic, G. (1976), "Measurement of structure borne wave intensity", *J. Sound Vib.*, **49**(2), 221-230.

Plunkett, R. and Lee, C.T. (1970), "Length optimization for constrained viscoelastic layer damping", *J. Acoust. Soc. Am.*, **48**(1), 150-161.

Sivasubramonium, B., Rao, G.V. and Krishnan, A. (1999), "Free vibration of longitudinally stiffened curved panels with cutout", *J. Sound Vib.*, **226**(1), 41-55.

Srivastava A.K.L. and Datta, P.K. (2006), "Elastic stability of souare stiffened plates with cutouts under biaxial loading", *Appl. Mech. Eng.*, **11**(2), 421-433.

Srivastava, A.K.L., Datta, P.K. and Sheikh, A.H. (2003), "Dynamic stability of stiffened plates subjected to non-uniform harmonic in-plane edge loading", *J. Sound Vib.*, **262**(5), 1171-1189.

Srivastava, A.K.L., Datta, P.K. and Sheikh, A.H. (2003), "Buckling and vibration of stiffened plates subjected to partial edge loading", *Int. J. Mech. Sci.*, **45**(1), 73-93.

Srivastava, A.K.L., Datta, P.K. and Sheikh, A.H. (2003), "Dynamic instability of stiffened plates with cutout subjected to in-plane uniform edge loadings", *Int. J. Struct. Stab. D.*, **3**(3), 391-403.

Xu, X.D., Lee, H.P. and Lu, C. (2004), "The structural intensities of composite plates with a hole", *Compos. Struct.,* **65**, 493-498.

Xu, X.D., Lee, H.P., Lu, C. and Guo, J.Y. (2005), "Streamline representation for vibration intensity fields", *J. Sound Vib*., **280**, 449-454.